**Atmospheric
Chemistry
and Physics
Discussions**

Comparison of tropospheric chemistry schemes for use within global models

K. M. Emmerson and M. J. Evans

School of Earth & Environment, University of Leeds, Leeds, LS2 9JT, UK

Correspondence to: K. Emmerson (k.emmerson@see.leeds.ac.uk)

Title Page

Abstract	Introduction
Conclusions	References
Tables	Figures

◄◄	►►
◄	►
Back	Close

Full Screen / Esc

Printer-friendly Version

Interactive Discussion

Abstract

Methane and ozone are two important climate gases with significant tropospheric chemistry. Within chemistry-climate and transport models this chemistry is simplified for computational expediency. We compare the state of the art Master Chemical Mechanism (MCM) with six tropospheric chemistry schemes (CRI-reduced, GEOS-CHEM and a GEOS-CHEM adduct, MOZART, TOMCAT and CBM-IV) that could be used within composition transport models. We test the schemes within a box model framework under conditions derived from a composition transport model and from field observations from a regional scale pollution event. We find that CRI-reduced provides much skill in simulating the full chemistry, yet with greatly reduced complexity. We find significant variations between the other chemical schemes, and reach the following conclusions. 1) The inclusion of a gas phase $N_2O_5+H_2O$ reaction in some schemes and not others is a large source of uncertainty in the inorganic chemistry. 2) There are significant variations in the calculated concentration of PAN between the schemes, which will affect the long range transport of reactive nitrogen in global models. 3) The representation of isoprene chemistry differs hugely between the schemes, leading to significant uncertainties on the impact of isoprene on composition. 4) Night-time chemistry is badly represented with significant disagreements in the ratio of NO_3 to NO_x. Resolving these four issues through further investigative laboratory studies will reduce the uncertainties within the chemical schemes of global tropospheric models.

1 Introduction

Anthropogenically induced climate change is largely caused by the changing composition of the atmosphere. Over the last 100 years the concentrations of carbon dioxide (CO_2), methane (CH_4) and ozone (O_3), have all increased significantly (IPCC, 2007). The associated radiative forcing is dominated by CO_2, however CH_4 and O_3 also play a significant role. To understand these changes and to predict the future atmospheric

composition, it is essential that we understand the photochemistry of the troposphere. Tropospheric photochemistry is dominated by a complex odd oxygen, hydrogen and nitrogen radical chemistry, coupled to the oxidation of volatile organic compounds (VOCs) (Logan et al., 1981). This presents various challenges. A complete and explicit

5 representation of tropospheric chemistry is limited by our understanding of the concentrations of gas phase species (often at very low concentrations) and their associated reactions. Even with our limited knowledge, the state of the science representation requires many thousands of species and tens of thousands of reactions. In the past decade, research has concentrated on producing large, chemically explicit, reaction

10 schemes. For example, Aumont et al. (2005) produced a scheme of 350 000 species and 2 million reactions. The Master Chemical Mechanism (Jenkin et al., 2003; Saunders et al., 2003; Bloss et al., 2005) contains approximately 5600 species and 13 500 reactions. Representing this level of chemical complexity within a global chemistry-climate model is beyond the computational resources currently available. Simplifica-

15 tions are required that retain the essential features of the chemistry whilst removing most of the complexity. Various methods have been used in the past in global models, with varying degrees of success. Simplifications involve reducing the number of VOCs considered and by lumping the carbon from the discarded species into representative surrogates.

20 In an earlier study, Derwent (1990) used 24 chemical schemes to compare modelled O_3 concentrations observed at sites across Europe. He determined that the more explicit schemes were able to capture the peak concentrations in O_3, peroxyacetylnitrate (PAN) and hydrogen peroxide (H_2O_2) more often than the highly parameterized schemes. The "PhotoComp" group was set up to provide a model intercomparison for

25 the Intergovernmental Panel on Climate Change, on modelling tropospheric HO_x cycling and O_3 production (Olsen et al., 1997). Box models from 21 research groups were run under a range of atmospheric conditions to investigate the differences in the gas phase photochemistry. No attempt was made to standardize complex and photolytic reaction rates. The source of resulting disparity in O_3 concentrations was found to be

Comparison of model chemistry schemes

K. M. Emmerson and M. J. Evans

mainly due to differences in the reaction rate of O_3 with HO_2. The problem was traced back to whether water dependence in the $HO_2+HO_2 \rightarrow H_2O_2$ reaction was included, and differing photolysis between models.

In this paper, six small and "reduced" schemes currently employed in composition transport models are compared to a "state of the science" explicit chemistry scheme. The aim is to evaluate the schemes under a range of different conditions and to identify areas of weakness.

2   The chemistry schemes

The MCM (version 3.1) is an explicit chemical scheme which degrades 135 primary VOCs into CO_2 and H_2O. The MCM contains approximately 5600 species and 13 500 reactions based on a predefined protocol (Jenkin et al., 2003; Saunders et al., 2003; Bloss et al., 2005). It was designed to provide regulatory controls on VOC emissions within the UK. The MCM has been tested against atmospheric measurements and smog chamber data (Jenkin and Hayman, 1999), and evaluated in urban (Emmerson et al., 2007, 2005), rural and marine modelling studies (Carslaw et al., 1999, 2001; Sommariva et al., 2004).

We use six smaller chemistry schemes in this study: CRI-reduced, GEOS-CHEM and a GEOS-CHEM extension, MOZART, TOMCAT and CBM-IV. We compare these to the explicit Master Chemical Mechanism (MCM). We note here that just because the MCM is classed as "state of the science" we are not assuming it is without limitations. Our scheme comparisons are therefore assumed to be relative to one another, rather than a comparison with "reality". The scheme sizes and capabilities are summarized in Table 1.

Based upon the MCM, the Common Representative Intermediates mechanism (CRI-mech) (Jenkin et al., 2002) is a reduction scheme based on the O_3 production potential of a species. A lumping methodology assigns large numbers of MCM species to generic intermediate species, which are then used to channel the chemistry into

smaller compounds such as formaldehyde (HCHO). These smaller species can then be treated using the MCM. The development of version 2 of CRI-mech, and a series of five reduced variants of the mechanism, has recently been reported (Jenkin et al., 2008; Watson et al., 2008). The most reduced variant (denoted "CRI v2-R5" in Wat-
5 son et al., 2008) contains 196 species and 555 reactions, and is used in this work (denoted "CRI-reduced"). CRI-reduced degrades 23 primary emitted VOCs including alkanes ≥C4, the aromatic compounds benzene, toluene and o-xylene, and biogenic compounds isoprene, α- and β-pinene. Given its size there is potential to use the CRI-reduced scheme within composition transport models in the future.

10 The GEOS-CHEM scheme (Bey et al., 2001; Evans and Jacob, 2005) was developed for inclusion in a global atmospheric chemistry-transport model using the Goddard Earth Observation System meteorology. It has 273 reactions and considers the oxidation of methane, ethane, propane, an alkene (nominally propene), a higher alkane (nominally butane), and isoprene. Additional chemical complexity has been
15 added to GEOS-CHEM to account for higher alkanes ≥C_4, biogenic species (α-pinene and limonene) and aromatic compounds (benzene, toluene and m-xylene) by Ito et al. (2007). This 490 reactions scheme also includes an explicit representation of hydroxyl alkyl nitrates produced rapidly from isoprene oxidation. We test this enhanced GEOS-CHEM scheme separately and name it GEOSito.

20 MOZART was developed by communities at NCAR in Colorado, the GFD Laboratory at Princeton and MPI at Hamburg (Horowitz et al., 2003). It has 158 reactions degrading alkanes ≤C_4, alkenes ≤C_3, 4 oxygenated compounds and isoprene. A lumped monoterpene compound has been included to add to the biogenic modelling capabilities.

25 The TOMCAT chemistry scheme (Chipperfield et al., 1993; Law et al., 1998; Stockwell and Chipperfield, 1999) contains 152 reactions and considers the oxidation of methane, ethane and propane. TOMCAT has been increased in recent years by the addition of the 34 reaction Mainz Isoprene Mechanism (Poschl et al., 2000). There is no representation for higher hydrocarbons or aromatic chemistry.

Comparison of model chemistry schemes

K. M. Emmerson and M. J. Evans

Title Page

Abstract	Introduction
Conclusions	References
Tables	Figures

|◄ | ►|

◄ | ►

Back | Close

Full Screen / Esc

Printer-friendly Version

Interactive Discussion

The CBM-IV scheme (Gery et al., 1989) is the smallest scheme tested in this work with 85 reactions, and is used for air pollution regulation. It considers the oxidation of lumped paraffin and olefin species, such as toluene and xylene, and includes isoprene. The CBM-IV is used within the GISS model (Shindell et al., 2003) and Tracer Model 3 (Houweling et al., 1998) to study tropospheric chemical dynamics.

3 The model framework

Each chemistry scheme is removed from the parent model and translated into the Kinetic PreProcessor (KPP) format (Sandu and Sander, 2006), which writes the ordinary differential equations to be integrated (available from (http://people.cs.vt.edu/~asandu/Software/Kpp). The chemistry is integrated forwards using a Rosenbrock solver (Hairer and Wanner, 1991). Photolysis rates have been calculated using the solar zenith angle based on the framework used for the MCM (Jenkin, 1997; Saunders et al., 2003). Trimolecular reactions are represented differently within each model. For simplicity these reaction rates have been taken from published IUPAC data (IUPAC, 2001). In order to provide a consistent assessment, we have switched off all heterogeneous chemistry. Both TOMCAT and MOZART include a "gas phase" reaction of $N_2O_5+H_2O$. The TOMCAT mechanism uses the IUPAC recommendation for the reaction rate of 2.5×10^{-22} molecule cm^{-3} s^{-1} (IUPAC, 2001). The MOZART mechanism suggests that the user define the reaction rate and we have opted to use the JPL recommendation of 2×10^{-21} molecule cm^{-3} s^{-1} (JPL, 2006) for comparison. These reactions are discussed later.

3.1 Boundary conditions

The chemistry schemes are run within a single box, forward in time for 120 h (5 days) starting from midnight. The choice of timescale is complex. Very long simulations would be unrealistic as the mixing of air masses would become a significant driver of

composition, whereas very short timescales would not test the ability of the chemistry to feedback significantly on itself. To fully evaluate all the appropriate timescales, a global model would have to be run for multiples of the methane lifetime (the longest lived species). This is beyond the numerical resources available and a compromise of 5 days is chosen.

The simplest assumption for a single box is to assume no external fluxes. This implies that no emissions, deposition nor mixing takes place. For some species this approximation leads to a significant deviation from reality over the 5 day integration. This is most notable for oxides of nitrogen where the rapid conversion of NO_x (defined as $NO+NO_2$) to NO_z (defined as all oxidized nitrogen species minus NO_x) can lead to unrealistic conditions. To counter this, we repeat simulations maintaining a constant concentration of NO_x^*. We define NO_x^* as the sum of $[NO]+[NO_2]+[NO_3]+2[N_2O_5]+[HONO]+[HO_2NO_2]$.

3.2 The simulations

The chemistry schemes should be capable of accurately simulating the chemistry of the atmosphere under the wide range of conditions found within the troposphere. Over the remote marine boundary layer, concentrations of anthropogenic pollutants are low, whereas over highly populated regions concentrations of pollutants are high; chemical processes are different in the warm tropics compared with the cold poles etc. The ideal reduced chemistry scheme should be able to simulate the chemistry under the range of conditions found through the troposphere.

We identify a reasonable and consistent range of concentrations based on the output of a composition transport model. However, the coarse resolution of the global model results in an underestimate of the maximum concentrations likely to occur in industrial regions during pollution events. In order to simulate a regional pollution event, concentrations are taken from a field program around London. Conditions from the global model and the London project are described below.

3.3 Global model conditions

An annual simulation (nominally the year 2004) of the GEOS-CHEM composition transport model (Bey et al., 2001) is used to prepare a range of appropriate initial conditions for the model simulations. The model is run at $4° \times 5°$ resolution with 30 vertical levels.

5 The monthly mean concentration of tracers for each grid box is then used for a principal components analysis. This transforms the information known about each grid box from being in "concentration space" to being represented as a series of components which describe the variability between species. For example, in most industrial gridboxes the concentrations of primarily emitted species such as CO, NO_x, and the hydrocarbons

10 all vary with time in a similar manner, whereas the composition of forested grid-boxes with high emissions of isoprene and other biogenically emitted VOCs vary in a similar manner. The first three principal components describe 75% of the compositional variability within the model. The first component represents the variation between clean and polluted regions, the second component represents a warm area versus cold dif-

15 ference and the third component represents a biogenically active versus a biogenically inactive region. The two gridboxes which exhibit the most extreme behaviour (i.e. have the highest and lowest values of the component) from within each of these first three principal components are selected and their monthly mean concentrations used as the initial conditions for these model simulations. Table 2 gives the locations of the grid

20 boxes and the conditions used. The different latitudes and days of year contribute to different photolytic conditions calculated within the model.

3.4 TORCH inputs and carbon lumping

Due to the spatial resolution of the GEOS-CHEM model, even the most anthropogenically polluted airmasses are less polluted than are observed in reality during a regional

25 pollution event. In order to test the model under conditions typical of very polluted airmasses, data are used from the Tropospheric Organic CHemistry (TORCH) field campaign which took place 25 miles north east of London, UK, during the summer of 2003,

amidst a heat wave and photochemical smog episode (Lee et al., 2006). We have model inputs for 12 long-chain and cyclic alkanes $\leq C_8$, 11 alkenes $\leq C_5$, 6 aromatics $\leq C_8$, 3 alcohols, isoprene and a range of small molecular weight aldehydes, acetylene and 1,3-butadiene (see Table 3). The MCM is the only chemistry scheme used here equipped to model the TORCH observations explicitly. Therefore some lumping of the carbon has been undertaken on a per carbon molecule basis to fit the other schemes, ensuring that the total initial concentration of reactive carbon (ppbC) in all the schemes is the same.

Table 3 shows the input concentrations for the average TORCH conditions along with the lumping taking place within the different schemes. Where schemes enable explicit representation, this is carried out. For all species which are not represented within a particular scheme, all alkanes are lumped into the highest alkane, all alkenes into the highest alkene, and all aromatics into the highest aromatic, maintaining the total mass of carbon. There are some exceptions, for example there is no alkene or aromatic representation in TOMCAT. Therefore, all alkenes and aromatics are lumped into propane on a per carbon basis (isoprene is treated separately). The MOZART scheme allows all alkane carbon into butane, but no aromatic representation means the aromatic carbon is lumped into propene. The CRI-reduced scheme allows for benzene, toluene, xylene, all alkanes and alkenes $\leq C_4$ to be treated explicitly; therefore all higher molecular weight compounds have been placed into butane or trans-but-2-ene where appropriate. For the GEOS-CHEM and GEOSito schemes the ethane, propane and isoprene concentrations are again taken from the observations, the ALK4 species is used to represent the remaining alkanes and the PRPE species is used to represent the remaining alkenes, alkynes and aromatics. In addition, the GEOSito scheme can deal separately with benzene and toluene. The CBM-IV mechanism allows ethane, propane, isoprene, toluene and xylene degradation, leaving the higher alkanes lumped into the PAR species, and the higher alkenes into the OLE species. Benzene has been lumped into the toluene species.

4 Diagnostics

The focus of this study is on chemistry schemes relevant for chemistry-climate simulations. Thus the emphasis is upon CH_4 and O_3. The long lifetime of CH_4 ($\sim$10 years) relative to the length of the simulations (5 days) makes a direct comparison of CH_4 less useful. The dominant sink for CH_4 in the atmosphere is the reaction of OH, thus we focus the comparison on the ability of the chemistry schemes to simulate OH. Ozone is another potent climate gas and also contributes to the oxidizing capacity of the atmosphere through production of the hydroxyl radical, OH. At ground level, O_3 also causes public health issues and leads to the destruction of plant material. Reactive nitrogen species (NO_x) play a central role in the chemistry of the troposphere. They are responsible for the catalytic production of O_3 and for the conversion of HO_2 to OH. Numerical models must have some skill in simulating the NO_x concentrations. In remote regions the source of NO_x is the decomposition of PAN which is formed in polluted regions from the oxidation of hydrocarbons in the presence of NO_x and subsequently exported to remote regions. During the night NO_3 acts as the dominant oxidant and needs to be considered. In this work we focus our comparisons on the ability of the various chemistry schemes on simulating the OH, O_3, NO_x, NO_3 and PAN concentrations.

Each of the chemistry schemes can be split into an "inorganic scheme" which considers essentially O_x-HO_x-NO_x-CO-CH_4 chemistry, and an "organic" scheme that considers the degradation of VOCs. We test the inorganic chemistry first on the belief that there should be little model variability between the schemes. We then test the full chemistry schemes.

5 Results

We first present the results using the six initial conditions derived from the principal components analysis of the GEOS-CHEM model. First the inorganic segments of the different chemistry schemes are tested with no boundary conditions, then the full

Title Page

Abstract | Introduction

Conclusions | References

Tables | Figures

◀ | ▶

◀ | ▶

Back | Close

Full Screen / Esc

Printer-friendly Version

Interactive Discussion

chemistry schemes are tested with no boundary conditions and finally the full chemistry schemes are tested with the constant NO_x^* boundary conditions. We tabulate the results in Table 4, to aid the reader in scheme comparisons with the MCM for O_3 production capabilities.

5.1 Inorganic schemes

This section compares the results when only the models' inorganic schemes are used. Other than CH_4, HCHO and CH_3OOH there is no reactive carbon in any of these initial conditions. Initially, comparisons highlighted a significant difference between TOM-CAT and MOZART, and the other schemes. This is diagnosed as being due to the gas phase reaction of $N_2O_5+H_2O$ that is included in the two schemes (optional in MOZART) and not the others. Figure 1 shows that the inclusion of the reaction in TOMCAT and MOZART leads to a ~20 ppb difference in O_3 over the 120 h for the industrial case, impacting on OH production and NO_x cycling. When this reaction is removed, we find much better agreement between the schemes (see Fig. 2). Although this reaction is in both the JPL and IUPAC recommendations there is some obvious doubt in the community over the rate, and this should be investigated by further collaboration. We remove this reaction from the MOZART and TOMCAT schemes in subsequent simulations.

Figure 2 shows results for all the chemistry schemes, showing OH, O_3 and NO_x concentrations over 5 days. In general the results are similar, however given our assumed knowledge on the state of the science with regard to the inorganic chemistry it is surprising that the models exhibit any significant differences. The CBM-IV and GEOS-CHEM models show significant deviations from the MCM run (our defined standard) in the industrial case (Fig. 2a). After 5 days we find differences in O_3 of up to ~8 ppb between the schemes. Using the industrial temperature of 299.7 K we calculate the differences in the scheme rates compared to the MCM: for example in the CBM-IV mechanism O_3+OH (−65%), NO_3+NO_2 (−39%) and O_3+HO_2 (+29%); In GEOS-CHEM O_3+NO (+14%). Much of this disagreement lies within differences between the IUPAC and JPL kinetics. If at this basic level the schemes do not agree, then we sus-

pect that inclusion of organic chemistry will make the calculated concentrations of OH, O_3 and NO_x diverge further. Future collaborative studies between the IUPAC and JPL kinetic data communities could yield a definitive set of rates for the inorganic chemistry.

5.2 Full chemistry, no boundary conditions

Figure 3 shows the same simulations but with the inclusion of initial conditions for the organic species. Resulting O_3 concentrations are given in Table 4. The CRI-reduced scheme emulates the MCM result very well. Differences between the other schemes largely exist in the simulations where NO_x and VOCs are high. For the "clean" regions simulated (Fig. 3b, d and f) the inclusion of the organic chemistry schemes lead to only small changes in the behaviour of the model. In these regions the concentrations of organic species are low and so it is not surprising that the inclusion of the organics is insignificant on our primary diagnostics (O_3 and OH). However, one notable difference is the generally lower NO_x produced by the CBM-IV mechanism with the inclusion of the organics. In Fig. 3b and d, variations in the PAN concentrations calculated by the CBM-IV scheme vary by up to a factor of 5. There is no acetone in CBM-IV and the PAN precursor CH_3CO_3 is produced from $CH_3CHO+NO_3$, which is inefficient at low NO_x concentrations. The two GEOS-CHEM models produce twice the MCM peak PAN concentrations after 5 days (Fig. 3b). At low PAN concentrations significant variations exist between models. PAN is able to transport reactive nitrogen to cleaner regions of the atmosphere, therefore the different abilities of the chemical schemes to calculate PAN lead to concerns that the oxidizing capacities downwind of our box model will vary significantly.

The biogenic case (Fig. 3e) shows significant variation with some schemes producing O_3 and some losing O_3. There is also a significant effect on the resulting OH concentrations. This suggests that there is no real consensus between models as to the impact of isoprene on the chemical system. Much of this debate hinges on the role of isoprene nitrates (Fiore et al., 2005; Ito et al., 2007; von Kuhlmann et al., 2004). Isoprene nitrates are formed through the reaction of NO with peroxy radicals formed

Comparison of model chemistry schemes

K. M. Emmerson and
M. J. Evans

from isoprene oxidation. Degradation of organic nitrates via reaction with OH returns either NO_x or HO_x at the first degradation step, but not both. If NO_x is returned to the chemical system, organic nitrates can act to transport 'reactivity' from the isoprene sources much as PANs do. The net effect being that O_3 concentrations can increase.

5　If on the other hand NO_x is not returned, then overall O_3 production is suppressed and O_3 loss can occur. Most schemes, with the exception of GEOSito and CBM-IV, will return the stored NO_x.

　　We test the sensitivity of the O_3 concentrations calculated between the two GEOS-CHEM schemes by varying the initial isoprene on a scale between 0.01 and 30 ppb.

10　The other inputs to the model were the same as the biogenic scenario inputs given in Table 2. The results (not shown) highlight the uncertainty in the chemistry of isoprene. The GEOS-CHEM run showed O_3 production from all initial inputs of isoprene. By contrast, the GEOSito scheme shows a distinct regime change from initial O_3 production for initial isoprene concentrations less than 2 ppb, to O_3 loss at initial isoprene

15　concentrations greater than 2 ppb. The most marked change in behaviour occurs at isoprene input concentrations between 0.1–1 ppb. The reason for this switch from O_3 production to loss in GEOSito is the availability of NO_x. When isoprene concentrations are in excess of 2 ppb the NO_x is held in the organic nitrates and not released. This test has emphasized the differences in the treatment of isoprene between schemes,

20　and underscores the fact that the chemistry of isoprene in the atmosphere is currently uncertain.

5.3　Full chemistry, with boundary conditions

We repeat the simulations with the constant NO_x^* boundary conditions and show the results in Fig. 4 and Table 4. By keeping the NO_x^* concentration constant, one of the

25　dominant feedbacks on the system is removed – that between the organic chemistry and the NO_x^* concentrations. The higher NO_x^* concentrations together with the lack of surface deposition in the simulations lead to significant O_3 production in most cases. In general these results look similar to previous experiments. The largest differences are

Comparison of model chemistry schemes

K. M. Emmerson and
M. J. Evans

seen in the biogenic case (Fig. 4e) where the range of OH, O_3 and NO_x concentrations are highest. The NO_x concentration in the cold simulations (Fig. 4c and f) drops slowly as NO_2 is converted to HO_2NO_2 (we do not initialize concentrations of HO_2NO_2).

Significant differences between model chemistry schemes are seen during the night. We show the NO_3 time series in Fig. 4 instead of PAN because the industrial and biogenic scenarios (Fig. 4a and e) exhibit near constant NO_x conditions during the day, with substantial conversion at night to NO_3 and N_2O_5. NO_3 concentrations can vary by factors of ~2 between models. Some of these differences can be attributed to the different O_3 concentrations calculated (which compare the rate of NO_3 production through NO_2+O_3), however other significant differences exist in the treatment of NO_3+VOC and NO_3+RO_2 reactions. These are most significant for the biogenic cases.

These uncertainties in night time chemistry have a range of implications for night time NO_x loss, nitrate aerosol production, secondary organic aerosol (SOA) production etc. Recently developed techniques for NO_3 and N_2O_5 measurement (Brown et al., 2006) will allow enhanced testing of night time chemistry schemes which should yield improvements.

5.4 Lumped chemistry using TORCH input data

As described earlier, the conditions derived from the global model underestimate the values likely to occur during a regional scale pollution event due to the spatial and temporal averaging. As computational resources increase, the spatial scale of models is likely to reduce. Thus the concentrations of species that will need to be simulated will increase. To produce simulations at the most polluted levels, observations from the TORCH 2003 summer campaign are used (Lee et al., 2006). The dataset used here represents the mean conditions observed during a regional pollution episode. The campaign was categorized by temperatures up to 312 K and significant regional scale air pollution. Peak measurements of O_3 at the TORCH site reached in excess of 110 ppb, and with CO concentrations of 520 ppb (Lee et al., 2006).

Figure 5 and Table 4 show results for the simulation for the average TORCH cam-

paign. We include results for an "inorganic" case (Fig. 5a) using TORCH measurements of CH_4, CO, NO_x and O_3 to investigate the impact of the organic carbon (Fig. 5b). We also show results including the constant NO_x^* boundary conditions (Fig. 5c).

For all simulations we notice a difference in the night-time chemistry in the OH and NO_x profiles, which is due to the treatment of NO_3 discussed in Sect. 5.3. Significant differences are also seen in the calculated O_3 between schemes, which is more pronounced with the inclusion of the organic scheme simulations due to the higher NO_x concentrations. The temporal variation in O_3 concentrations differ between the inorganic and organic simulations, with a pattern of loss early on for the inorganic test (Fig. 5a), and enhanced production after 75 h reflecting suppression of O_3 production by NO_x early in the simulation followed by enhanced O_3 production later in the simulation as NO_x decreases. By contrast there is production of O_3 from the start in the full chemistry simulations with no boundary conditions (Fig. 5b). Inclusion of the boundary conditions results in a loss of O_3 from the start of the run (Fig. 5c). In this respect the shape of the inorganic TORCH run combines elements from both full chemistry tests. The input concentrations for both full chemistry tests are the same, but inclusion of the extra NO_x^* through the boundary conditions has reduced the overall O_3 and OH concentrations compared with Fig. 5b.

These tests have been designed to investigate how well small chemistry schemes simulate increasingly complex tropospheric input scenarios. Therefore the smaller chemistry schemes have the same concentrations of carbon input, but it has been lumped into smaller molecular weight VOCs (Table 3). Overall the CRI-reduced scheme is an excellent proxy for the MCM. The smaller TOMCAT scheme shows good agreement with the MCM in predicting both OH and O_3 concentrations, even though all the carbon is lumped into the propane species. Such simplifications of the chemistry are necessary if global transport models require a full representation of the composition of the troposphere in future.

6   Conclusions

Large explicit schemes of atmospheric chemistry such as the MCM are too complex to be considered for 3D global chemistry-climate models. However, they can be used as benchmarks against which to compare smaller reduced schemes which are suitable for inclusion. Six chemical schemes have been removed from their parent model environments and run in a simple box model with specific input concentrations. A variety of tests performed here highlight problems, both simple and complex, with the schemes used here. We find several main conclusions:

1. The CRI-reduced scheme contains 4% of the number of reactions in the MCM, yet has proved to be an excellent MCM surrogate as highlighted by the resulting O_3 concentrations from all the simulations in Table 4. We expect increased use of such reduced schemes in future, where the chemistry can be traced back to larger comprehensive schemes.

2. The gas phase reaction between N_2O_5 and H_2O is included in TOMCAT and MOZART but not in the other schemes. This leads to significant differences in the concentration of NO_x. There appears to be confusion over the existence and rate of this reaction and laboratory studies should be undertaken to evaluate its significance. When this reaction is removed, small differences still exist in the inorganic chemistry schemes of the different models due to reaction rate inconsistencies. This suggests that a future effort should be to reduce some of the differences between model inorganic schemes.

3. PAN concentrations calculated in the full chemistry test with no boundary conditions (Sect. 5.2) varied by up to a factor of 5 under clean conditions (Fig. 3b). The CBM-IV scheme, the smallest tested in this work, excludes acetone and thus has significant problems simulating PAN. Whilst the other mechanisms do include acetone, the rate at which the PAN precursor, CH_3CO_3 is produced varies. As PAN is able to transport reactive nitrogen to cleaner regions of the atmosphere,

these differences may impact on the oxidizing capacity in remote regions.

4. When organic chemistry is included, the differences between the models increase compared to the inorganic scheme alone. We find that these differences are most pronounced under high biogenic VOC loadings where even the sign of the impact of isoprene on O_3 varies between the schemes. We identify the treatment of isoprene derived organic nitrates as the dominant cause of these discrepancies. Given that isoprene emission and chemistry is a critical composition-climate feedback we believe that resolving this issue should be of central importance to future research effort.

5. The night time chemistry also shows considerable differences between the schemes. Significant variations in NO_3 concentrations occur in simulations with high VOCs. The NO_3 produced varied by a factor of $\sim$2, and can be attributed to differences in the treatment of NO_3+VOC and NO_3+RO_2 reactions. These variations will impact night time oxidation, nitrate aerosol production and NO_x concentrations.

In conclusion, we would like to draw attention to the differences that exist within the current generation of chemistry schemes. These differences can impact on the long range transport of species and aerosol production. This "chemistry uncertainty" is in addition to current model uncertainties due to dynamics, emissions, transport etc. Further laboratory kinetic studies will reduce this uncertainty. Advances in available computer time will soon allow moderately complex schemes such as CRI-reduced, which are based on reductions of explicit schemes, to be included in composition transport and composition climate models. Global model comparisons between simulations using complex chemistries and simpler chemistry will allow for a full evaluation of scheme capabilities.

Comparison of model chemistry schemes

K. M. Emmerson and
M. J. Evans

Title Page

Abstract | Introduction

Conclusions | References

Tables | Figures

◄ | ►

Back | Close

Full Screen / Esc

Printer-friendly Version

Interactive Discussion

References

Aumont, B., Szopa, S., and Madronich, S.: Modelling the evolution of organic carbon during its gas-phase tropospheric oxidation: development of an explicit model based on a self generating approach, Atmos. Chem. Phys., 5, 2497–2517, 2005, http://www.atmos-chem-phys.net/5/2497/2005/.

Bey, I., Jacob, D. J., Yantosca, R. M., et al.: Global modelling of tropospheric chemistry with assimilated meteorology: model description and evaluation, J. Geophys. Res., 106, 23 073–23 095, 2001.

Bloss, C., Wagner, V., Jenkin, M. E., Volkamer, R., Bloss, W. J., Lee, J. D., Heard, D. E., Wirtz, K., Martin-Reviejo, M., Rea, G., Wenger, J. C., and Pilling, M. J.: Development of a detailed chemical mechanism (MCMv3.1) for the atmospheric oxidation of aromatic hydrocarbons, Atmos. Chem. Phys., 5, 641–664, 2005, http://www.atmos-chem-phys.net/5/641/2005/.

Brown, S. S., Ryerson, T. B., Wollny, A. G., Brock, A. G., Peltier, R., Sullivan, A. P., Weber, R. J., Dube, W. P., Trainer, M., Meagher, J. F., Fehsenfeld, F. C., and Ravishankara, A. R: Variability in nocturnal nitrogen oxide processing and its role in regional air quality, Science, 311, 67–70, 2006.

Carslaw, N., Creasey, D. J., Heard, D. E., Lewis, A. C., McQuaid, J. B., Pilling, M. J., Monks, P. S., Bandy, B. J., and Penkett, S. A.: Modelling OH, HO_2 and RO_2 radicals in the marine boundary layer. 1. Model construction and comparison with field measurements, J. Geophys. Res., 104, 30 241–30 255, 1999.

Carslaw N., Creasey, D. J., Harrison, D., Heard, D. E., Hunter, M. C., Jacobs, P. J., Jenkin, M. E., Lee, J. D., Lewis, A. C., Pilling, M. J., Saunders, S. M., and Seakins, P. W.: Modelling OH and HO_2 radicals in a forested region of north-western Greece, Atmos. Environ., 35, 4725–4737, 2001.

Chipperfield, M. P., Cariolle, D., Simon, P., Ramaroson, R., and Lary, D. J.: a three dimensional modelling study of trace species in the Arctic lower stratosphere during winter 1989–1990, J. Geosphys. Res., 98, 7199–7218, 1993.

Comparison of model chemistry schemes

K. M. Emmerson and M. J. Evans

Derwent, R. G.: Evaluation of a number of chemical mechanisms for their application in models describing the formation of photochemical ozone in Europe, Atmos. Environ., 24A, 2615–2624, 1990.

Emmerson, K. M., Carslaw, N., Carpenter, L. J., Heard, D. E., Lee, J. D., and Pilling, M. J.: Urban Atmospheric Chemistry during the PUMA Campaign, 1: Comparison of Modelled OH and HO_2 Concentrations with Measurements, J. Atmos. Chem., 52, 2, 143–164, 2005.

Emmerson, K. M., Carslaw, N., Carslaw, D. C., Lee, J. D., McFiggans, G., Bloss, W. J., Gravestock, T., Heard, D. E., Hopkins, J., Ingham, T., Pilling, M. J., Smith, S. C., Jacob, M., and Monks, P. S.: Free radical modelling studies during the UK TORCH Campaign in Summer 2003, Atmos. Chem. Phys., 7, 167–181, 2007,
http://www.atmos-chem-phys.net/7/167/2007/.

Evans, M. J and Jacob, D. J.: Impact of new laboratory studies of N_2O_5 hydrolysis on global model budgets of tropospheric nitrogen oxides, ozone and OH, Geophys. Res. Lett., 32, L09813, doi:10.1029/2005GL022469, 2005.

Fiore, A. M., Horowitz, L. W., Purves, D. W., et al.: Evaluating the contribution of changes in isoprene emissions to surface ozone trends over the eastern United States, J. Geosphys. Res., 110, D12303, doi:10.1029/2004JD005485, 2005.

Gery, M. W., Whitten, G. Z., Killus, J. P., and Dodge, M. C.: A Photochemical Kinetics Mechanism for Urban and Regional Scale Computer Modeling, J. Geophys. Res., 94, 925–956, 1989.

Hairer, E. and Wanner, G.: Solving Ordinary Differential Equations II Stiff and Differential-Algebraic Problems, Springer-Verlag, Berlin, 1991.

Horowitz, L. W., Walters, S., Mauzerall, D. L., et al.: A global simulation of tropospheric ozone and related tracers: description and evaluation of MOZART version 2, J. Geophys. Res., 108(D24), 4784, doi:10.1029/2002JD002853, 2003.

Houweling, S., Dentener, F., and Lelieveld, J.: The impact of nonmethane hydrocarbon compounds on tropospheric photochemistry, J. Geophys. Res., 103, 10 673–10 696, 1998.

Ito, A., Sillman, S., and Penner, J. E.: Effects of additional nonmethane volatile organic compounds, organic nitrates, and direct emissions of oxygenated organic species on global tropospheric chemistry, J. Geophys. Res., 112, D06309, doi:10.1029/2005JD006556.2007.

IPCC: Climate Change 2007: The Physical Science Basis, Contribution of Working Group I to the Fourth Assessment Report of the Intergovernmental Panel on Climate Change, edited by: Solomon, S., Qin, D., Manning, M., Chen, Z., Marquis, M., Averyt, K. B., Tignor, M., and

Miller, H. L., Cambridge University Press, Cambridge, United Kingdom and New York, NY, USA, 996 pp., 2007.

IUPAC: Summary of evaluated kinetic and photochemical data for atmospheric chemistry, IUPAC subcommittee for Gas Kinetic Data Evaluation, 2001.

5 Jenkin M. E., Saunders S. M., Derwent R. G., and Pilling M. J.: Development of a reduced speciated VOC degradation mechanism for use in ozone models, Atmos. Environ., 36, 4725–4734, 2002.

Jenkin, M. E., Saunders, S. M., Wagner, V., and Pilling, M. J.: Protocol for the development of the Master Chemical Mechanism, MCM v3 (Part B): tropospheric degradation of aromatic

10 volatile organic compounds, Atmos. Chem. Phys., 3, 181–193, 2003, http://www.atmos-chem-phys.net/3/181/2003/.

Jenkin, M. E and Hayman, G. D.: Photochemical ozone creation potentials for oxygenated volatile organic compounds: sensitivity to variations in kinetic and mechanistic parameters, Atmos. Environ., 33(8), 1275–1293, 1999.

15 Jenkin, M. E., Watson, L. A., Utembe, S. R., and Shallcross, D. E.: A Common Representative Intermediates (CRI) mechanism for VOC degradation – Part 1: Gas phase mechanism development, Atmos. Environ., 42, 7185–7195, doi:10.1016/j.atmosenv2008.07.028, 2008.

JPL: Chemical kinetics and photochemical data for use in atmospheric studies, Evaluation number 15, California Institute of Technology, Pasadena, CA, 2006.

20 Law, K. S., Plantevin, P.-H., Shallcross, D. E., Rogers, H. L., Pyle, J. A., Grouhel, C., Thouret, V., and Marenco, A.: Evaluation of modeled O3 using Measurements of Ozone by Airbus In-Service Aircraft (MOZAIC) data, J. Geophys. Res., 103, 25 721-25 737, 1998.

Lee, J. D., Lewis, A. C., Monks, P. S., et al.: Ozone photochemistry and elevated isoprene during the UK heatwave of August 2003, Atmos. Environ., 40, 7598–7613, 2006.

25 Logan, J. A., Prather, M. J., Wofsy, S. C., and McElroy, M. B.: Tropospheric Chemistry: A Global Perspective, J. Geophys. Res., 86(C8), 7210–7254, 1981.

O'Connor, F. M., Law, K. S., Pyle, J. A., Barjat, H., Brough, N., Dewey, K., Green, T., Kent, J., and Phillips, G.: Tropospheric ozone budget: regional and global calculations, Atmos. Chem. Phys. Discuss., 4, 991–1036, 2004,

30 http://www.atmos-chem-phys-discuss.net/4/991/2004/.

Olsen, J., Prather, M., Berntsen, T., et al.: Results from the Intergovernmental Panel on Climatic Change Photochemical Model Intercomparison (Photocomp), J. Geophys. Res., 102, 5979–5991, 1997.

Poschl, U., von Kuhlmann, R., Poisson, N., and Crutzen, P. J.: Development and intercomparison of condensed isoprene oxidation mechanisms for global atmospheric modelling, J. Atmos. Chem., 37, 29–52, 2000.

Sandu, A. and Sander, R.: Technical note: Simulating chemical systems in Fortran90 and Matlab with the Kinetic PreProcessor KPP-2.1, Atmos. Chem. Phys., 6, 187–195, 2006, http://www.atmos-chem-phys.net/6/187/2006/.

Saunders, S. M., Jenkin, M. E., Derwent, R. G., and Pilling, M. J.: Protocol for the development of the Master Chemical Mechanism, MCM v3 (Part A): tropospheric degradation of non-aromatic volatile organic compounds, Atmos. Chem. Phys., 3, 161–180, 2003, http://www.atmos-chem-phys.net/3/161/2003/.

Shindell, D. T., Faluvegi, G., and Bell, N.: Preindustrial-to-present-day radiative forcing by tropospheric ozone from improved simulations with the GISS chemistry-climate GCM, Atmos. Chem. Phys., 3, 1675–1702, 2003, http://www.atmos-chem-phys.net/3/1675/2003/.

Sommariva, R., Haggerstone, A.-L., Carpenter, L. J., Carslaw, N., Creasey, D. J., Heard, D. E., Lee, J. D., Lewis, A. C., Pilling, M. J., and Zádor, J.: OH and HO2 chemistry in clean marine air during SOAPEX-2, Atmos. Chem. Phys., 4, 839–856, 2004, http://www.atmos-chem-phys.net/4/839/2004/.

Stockwell, D. Z. and M. J. Chipperfield.: A tropospheric chemical transport model: development and validation of the model transport schemes, Q. J. Roy. Meteor. Soc., 125, 1747–1783, 1999.

Szopa, S., Aumont, B., and Madronich, S.: Assessment of the reduction methods used to develop chemical schemes: building of a new chemical scheme for VOC oxidation suited to three-dimensional multiscale HO_x-NO_x-VOC chemistry simulations, Atmos. Chem. Phys., 5, 2519–2538, 2005, http://www.atmos-chem-phys.net/5/2519/2005/.

von Kuhlmann, R., Lawrence, M. G., Pöschl, U., and Crutzen, P. J.: Sensitivities in global scale modeling of isoprene, Atmos. Chem. Phys., 4, 1–17, 2004, http://www.atmos-chem-phys.net/4/1/2004/.

Watson, L. A., Shallcross, D. E., Utembe, S. R., and Jenkin, M. E.: A Common Representative Intermediates (CRI) mechanism for VOC degradation – Part 2: Gas phase mechanism reduction, Atmos. Environ., 42, 7196–7204, doi:10.1016/j.atmosenv.2008.07.034, 2008.

Wu, S., Mickley, L. J., Jacob, D. J., et al.: Why are there large differences between

Title Page

Abstract | Introduction

Conclusions | References

Tables | Figures

◄◄ | ►►

◄ | ►

Back | Close

Full Screen / Esc

Printer-friendly Version

Interactive Discussion

models in global budgets of tropospheric ozone?, J. Geophys. Res., 112, D05302, doi:10.1029/2006JD007801, 2007.

Comparison of model chemistry schemes

K. M. Emmerson and
M. J. Evans

Title Page

Abstract | Introduction

Conclusions | References

Tables | Figures

◄◄ | ►►

◄ | ►

Back | Close

Full Screen / Esc

Printer-friendly Version

Interactive Discussion

Table 1. The chemical mechanisms. Note that only tropospheric reactions are used in this study. Number of reactions required for the (M) = full chemistry test and (T) = TORCH tests.

	Reactions	No. of Species	Model Chemistry Includes…	Notes
MCM	13500 766 (M) 6502 (T)	5600 248 (M) 2241 (T)	135 VOCs including 22 alkanes $\leq C_{12}$, 16 alkenes $\leq C_6$, 6 aldehydes, 18 aromatics, isoprene, α- and β-pinene	The benchmark scheme
CRI-reduced	555	196	23 VOCs including alkanes $\leq C_4$, alkenes $\leq C_4$, 9 oxygenated compounds, benzene, toluene, o-xylene, isoprene, α- and β-pinene	4% of the size of the MCM
GEOSito	490	179	alkanes $\leq C_8$, alkenes $\leq C_4$, 11 oxygenated compounds, benzene, toluene, m-xylene, isoprene, α- and β-pinene	Ito et al. (2007) extended GEOS-CHEM mechanism
GEOS-CHEM	273	93	alkanes $\leq C_3$, alkenes $\leq C_4$, 9 oxygenated compounds, isoprene	
MOZART	158	63	alkanes $\leq C_4$, alkenes $\leq C_3$, acetylene, acetaldehyde, acetone, methanol, isoprene and lumped monoterpenes	
TOMCAT	152	58	Ethane, propane, acetylene, acetaldehyde, acetone, methanol and isoprene	Includes Mainz Isoprene Mechanism (Poschl et al., 2000)
CBM-IV	85	47	Ethene, isoprene, lumped parafins, olefins, aldehydes and aromatics	

Table 2. Input values (ppb, except H_2O which is $\times 10^{17}$ molecule cm^{-3}), from the principle component analysis.

	Industrial	Clean	Cold, Dry	Hot, Wet	Biogenic	Non-biogenic
Lon (° E)	100	−120	−45	−140	−145	−160
Lat (° N)	18	−30	−6	−10	26	−75
Julian Day No.	105	45	285	345	195	365
Pressure (hPa)	982.6	941.6	136.6	982.6	982.6	136.6
Temp (K)	299.7	299.4	214.4	302.7	302.5	214.3
H_2O	3.9	5.7	0.01	6.8	5.3	0.01
CH_4	1700.0	1700.0	1700.0	1700.0	1700.0	1700.0
CO	956.5	58.4	87.6	56.9	217.7	56.1
NO_2	3.6	0.003	0.58	0.002	0.12	0.14
O_3	63.3	19.0	86.3	13.3	10.5	93.9
H_2O_2	11.0	1.7	0.05	1.5	8.5	0.02
HNO_3	2.8	0.07	0.5	0.04	0.2	0.2
C_2H_6	5.6	0.2	0.9	0.2	0.6	0.3
C_3H_8	1.4	0.003	0.2	0.002	0.09	0.02
C_5H_8	0.3	–	–	–	6.7	–
HCHO	6.0	0.4	0.06	0.4	4.8	0.02
CH_3CHO	3.0	0.004	0.007	0.004	3.8	0.0006
PAN	1.0	0.00008	0.2	0.0003	0.04	0.03

Table 3. Division of species into lumped compounds within the full chemistry scheme tests. TORCH input concentrations, ppb, except H_2O in units $\times 10^{17}$ molecule cm^{-3}. "Me" is a methyl group. Chemical species are named using the methodology adopted by each mechanism.

MCM	AVE	CRI-reduced	GEOSito	GEOS-CHEM	MOZART	TOMCAT	CBM-IV
H_2O	3.69	H_2O	H_2O	H_2O	H_2O	H_2O	H_2O
CO	20.30	CO	CO	CO	CO	CO	CO
NO	2.83	NO	NO	NO	NO	NO	NO
NO_2	10.50	NO_2	NO_2	NO_2	NO_2	NO_2	NO_2
PAN	0.24	PAN	PAN	PAN	PAN	PAN	PAN
O_3	34.30	O_3	O_3	O_3	O_3	O_3	O_3
C_2H_6	2.36	C_2H_6	C_2H_6	C_2H_6	C_2H_6	C_2H_6	PAR
C_2H_4	0.57	C_2H_4	ETHE	PRPE	C_2H_6	C_2H_6	ETH
C_3H_8	1.23	C_3H_8	C_3H_8	C_3H_8	C_3H_8	C_3H_8	PAR
C_3H_6	0.18	C_3H_6	PRPE	PRPE	C_3H_6	C_3H_8	OLE
IC_4H_{10}	0.34	NC_4H_{10}	ALK4	ALK4	C_4H_{10}	C_3H_8	PAR
NC_4H_{10}	0.64	NC_4H_{10}	ALK4	ALK4	C_4H_{10}	C_3H_8	PAR
C_2H_2	0.46	C_2H_2	ETHE	PRPE	C_2H_6	C_2H_2	OLE
t-but-2-ene	0.01	t-but-2-ene	BUTE	PRPE	C_3H_6	C_3H_8	OLE
But-1-ene	0.04	t-but-2-ene	PRPE	PRPE	C_3H_6	C_3H_8	OLE
Me-propene	0.04	t-but-2-ene	PRPE	PRPE	C_3H_6	C_3H_8	OLE
c-but-2-ene	0.01	t-but-2-ene	PRPE	PRPE	C_3H_6	C_3H_8	OLE
C_5H_{12}	0.30	NC_4H_{10}	ALK4	ALK4	C_4H_{10}	C_3H_8	PAR
C_4H_6	0.02	t-but-2-ene	PRPE	PRPE	C_3H_6	C_3H_8	OLE
t-pent-2-ene	0.01	t-but-2-ene	PRPE	PRPE	C_3H_6	C_3H_8	OLE
pent-1-ene	0.01	t-but-2-ene	PRPE	PRPE	C_3H_6	C_3H_8	OLE
Me-2-but-1-ene	0.02	t-but-2-ene	PRPE	PRPE	C_3H_6	C_3H_8	OLE
Me-2-but-2-ene	0.01	t-but-2-ene	PRPE	PRPE	C_3H_6	C_3H_8	OLE
c-pent-2-ene	0.01	t-but-2-ene	PRPE	PRPE	C_3H_6	C_3H_8	OLE
di-Me-butane	0.10	NC_4H_{10}	ALK4	ALK4	C_4H_{10}	C_3H_8	PAR
c-hexane	0.03	NC_4H_{10}	ALK7	ALK4	C_4H_{10}	C_3H_8	PAR
Me-2-pentene	0.11	t-but-2-ene	ALK7	PRPE	C_3H_6	C_3H_8	OLE
Me-3-pentene	0.11	t-but-2-ene	ALK7	PRPE	C_3H_6	C_3H_8	OLE
C_6H_{14}	0.06	NC_4H_{10}	ALK7	ALK4	C_4H_{10}	C_3H_8	PAR
C_5H_8	0.12	C_5H_8	ISOP	ISOP	C_5H_8	C_5H_8	ISOP
C_7H_{16}	0.03	NC_4H_{10}	ALK7	ALK4	C_4H_{10}	C_3H_8	PAR
C_6H_6	0.19	C_6H_6	BENZ	PRPE	C_3H_6	C_3H_8	TOL
C_8H_{18}	0.04	NC_4H_{10}	ALK7	ALK4	C_4H_{10}	C_3H_8	PAR
C_7H_8	0.34	C_7H_8	TOLU	PRPE	C_3H_6	C_3H_8	TOL
Ethylbenzene	0.06	o-xylene	XYLE	PRPE	C_3H_6	C_3H_8	XYL
m-xylene	0.07	o-xylene	XYLE	PRPE	C_3H_6	C_3H_8	XYL
p-xylene	0.07	o-xylene	XYLE	PRPE	C_3H_6	C_3H_8	XYL
o-xylene	0.05	o-xylene	XYLE	PRPE	C_3H_6	C_3H_8	XYL
CH_3CHO	2.24	CH_3CHO	ALD2	ALD2	MeCHO	MeCHO	ALD2
CH_3OH	1.34	CH_3OH	MOH	MOH	MeOH	MeOH	OLE
CH_3COCH_3	1.68	CH_3COCH_3	ACET	ACET	Me2CO	Me2CO	OLE
MACR	0.03	t-but-2-ene	MACR	MACR	MACR	MACR	OLE
C_2H_5OH	1.11	C_2H_5OH	EOH	EOH	C_3H_8	C_3H_8	OLE
npropanol	0.09	C_2H_5OH	ROH	ROH	C_3H_8	C_3H_8	OLE
HCHO	1.63	HCHO	CH2O	CH2O	HCHO	HCHO	FORM

19981

Comparison of model chemistry schemes

K. M. Emmerson and
M. J. Evans

Table 4. MCM O_3 concentrations (ppb) after 120 h box model runs, with the corresponding results from all other schemes displayed as +/−ppb. NB = no boundary conditions. WB = with boundary conditions. T = TORCH.

| Test and corresponding figure	MCM	CRI-reduced	GEOSito	GEOSCHEM	MOZART	TOMCAT	CBM-IV
Inorganic							
2a. indus	81.32	−0.04	−1.76	−7.03	−3.55	−1.02	−8.33
2b. clean	10.35	0.00	0.05	−0.62	−0.59	−0.16	−0.20
2c. cold	86.62	0.06	0.12	0.09	0.20	0.09	0.03
2d. hot	7.36	0.00	0.05	−0.42	−0.41	−0.12	−0.11
2e. bio	14.44	0.00	−0.12	−0.85	−0.61	−0.49	−0.54
2f. n-bio	93.76	0.35	0.38	0.32	0.41	0.38	0.29
Full Chem NB							
3a. indus	89.98	−0.98	−3.23	−9.76	−4.70	−1.43	−12.50
3b. clean	10.35	0.00	0.07	−0.61	−0.57	−0.11	−0.41
3c. cold	86.73	0.09	0.12	0.12	0.20	0.12	0.09
3d. hot	7.35	0.00	0.05	−0.42	−0.41	−0.11	−0.30
3e. bio	19.41	−1.28	−13.70	−5.28	0.04	−1.93	−14.07
3f. n-bio	93.76	0.35	0.38	0.32	0.41	0.38	0.29
Full Chem WB							
4a. indus	235.39	0.00	−3.55	−31.41	0.78	−2.78	−12.21
4b. clean	70.54	−0.29	2.49	−3.67	15.14	2.86	−3.26
4c. cold	87.09	−0.29	−0.26	−0.29	−0.18	−0.26	−0.29
4d. hot	42.37	−0.17	1.57	−1.56	15.02	1.03	−0.25
4e. bio	177.79	−0.62	−18.30	−35.33	19.79	−8.57	−34.71
4f. n-bio	94.11	0.03	0.06	−0.03	0.06	0.03	−0.03
TORCH							
5b. NB	67.39	0.12	17.60	2.53	10.74	12.25	−17.56
5c. WB	27.59	−0.65	10.12	−9.93	8.14	3.57	−6.01
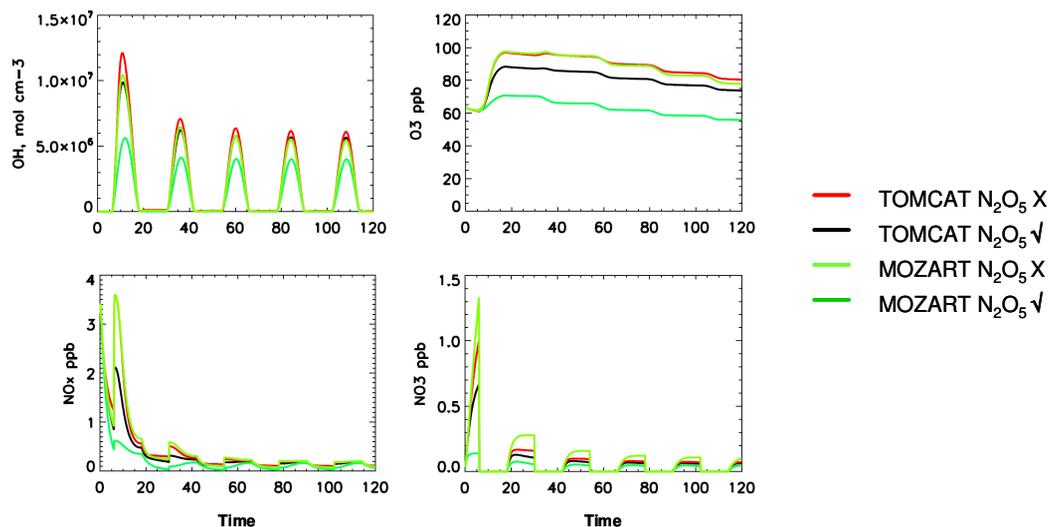
Fig. 1. Inorganic scheme 120 h run to show differences in OH, O_3, NO_x and NO_3 between the TOMCAT and MOZART schemes with the gas phase $N_2O_5 + H_2O$ reaction switched on ($\sqrt{}$) and off (X). Initial conditions for the industrial scenario are used (Table 2).
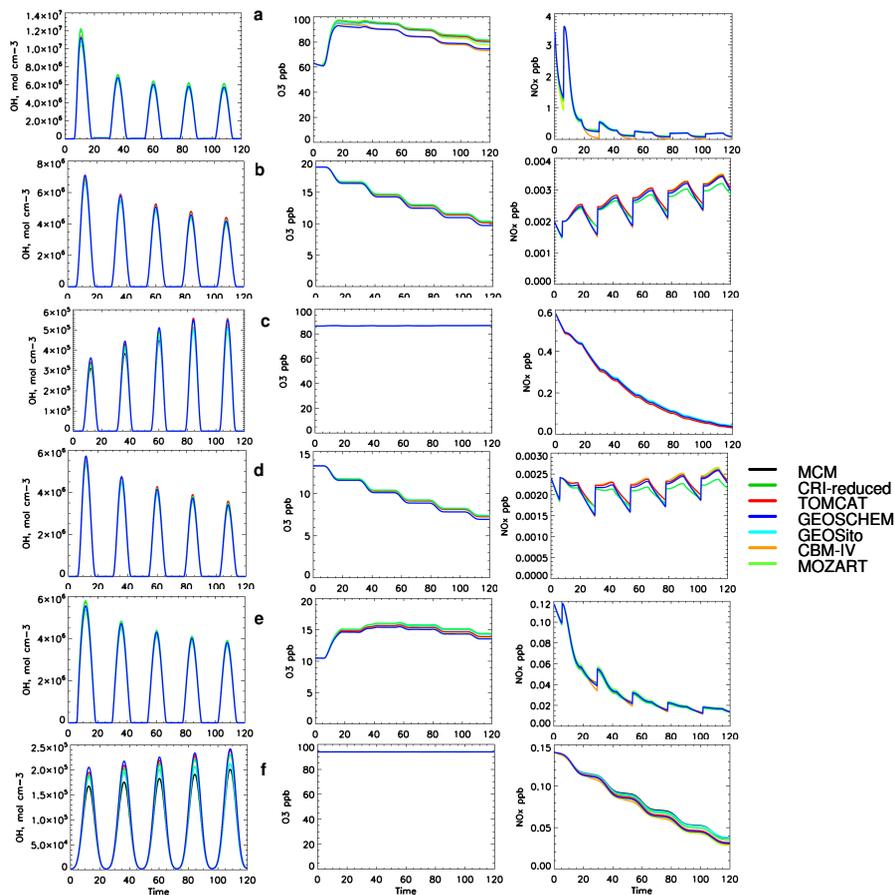
Fig. 2. Inorganic 120 h run without boundary conditions for OH (left), O_3 (middle) and $NO_x = NO + NO_2$ (right). a = industrial, b = clean, c = cold&dry, d = hot&wet, e = biogenic, f = non-biogenic.
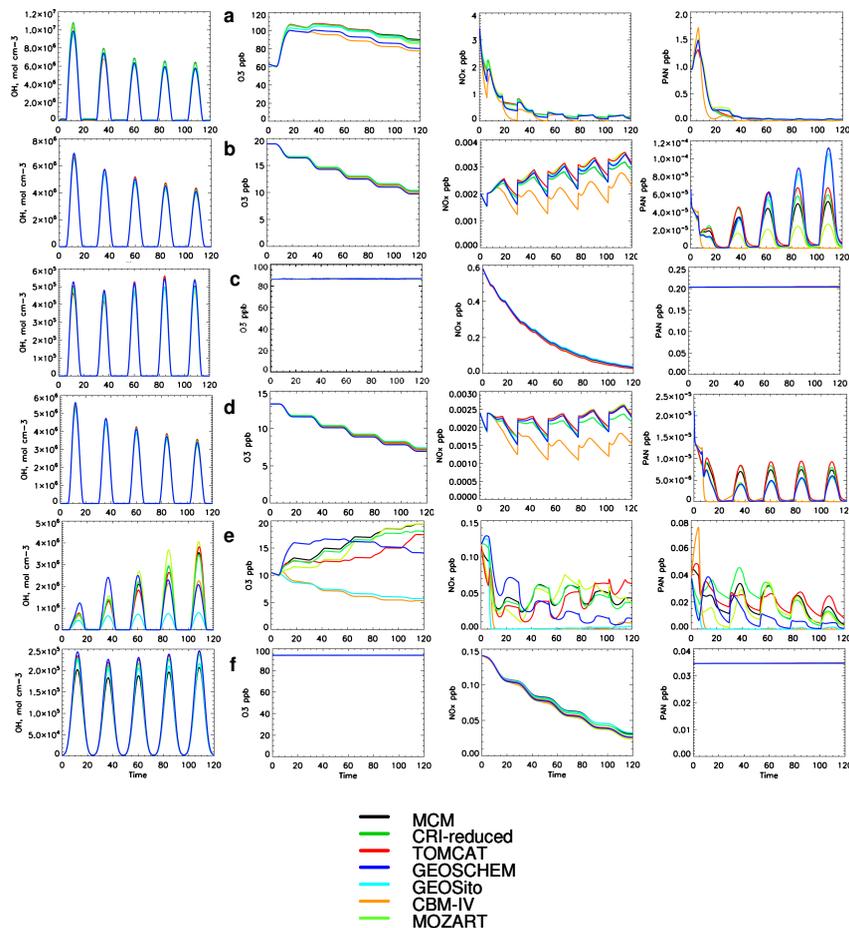
Fig. 3. Full chemistry scheme 120 h run with no boundary conditions. From left, OH, O_3, $NO_x=NO+NO_2$ and PAN. a = industrial, b = clean, c = cold&dry, d = hot&wet, e = biogenic, f = non-biogenic.
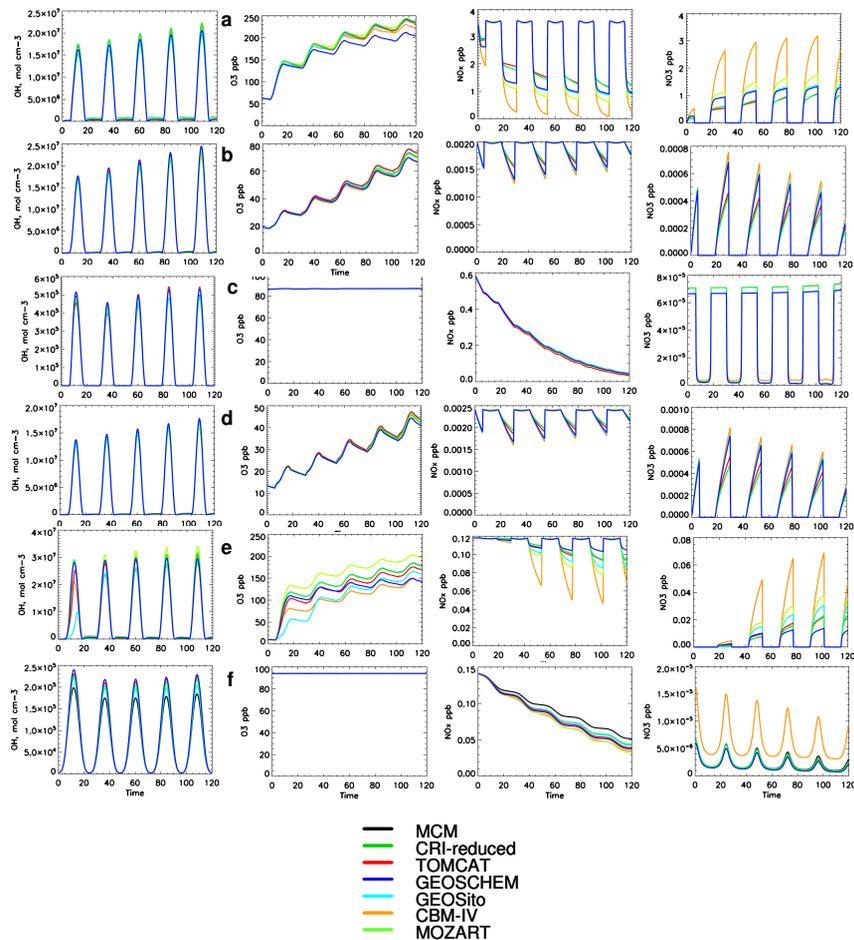
Fig. 4. Full chemistry scheme 120 h run including boundary conditions. From left OH, O_3, $NO_x = NO+NO_2$ and NO_3. a = industrial, b = clean, c = cold&dry, d = hot&wet, e = biogenic, f = non-biogenic.
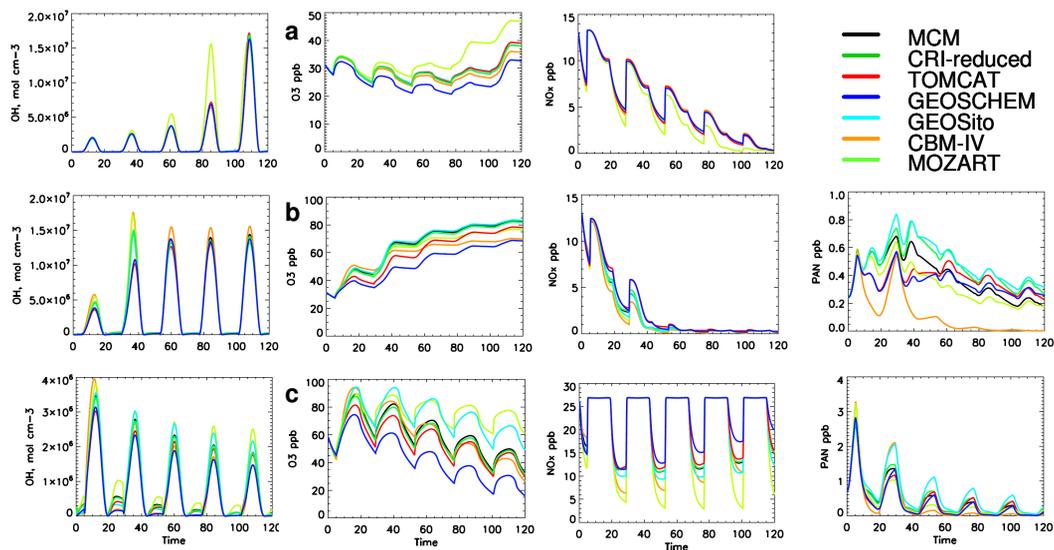
Fig. 5. Average TORCH campaign input data for 120 h run showing from left OH, O_3, $NO_x = NO + NO_2$ and PAN (not for inorganic run). a = inorganic chemistry only b = full chemistry without boundary conditions, c = full chemistry including boundary conditions.